Simulation of Fluid Flow and Heat Transfer Enhancement of Nano Fluids Past In-Line Tube Bank

Elhassen A. A. Omer, Moayed M. Wadan, Ahmed. A. Mami and Amer A. Alsharef

Mechanical Engineering Department, Faculty of Engineering, Zawia University

Abstract

Numerical investigation of heat transfer enhancement over an inline tube bank for turbulent flow of nanofluid is presented. Conservation equation of mass, momentum, energy and k – epsilon model under steady state have been solved using ANSYS Fluent. Heat transfer characteristic and flow over tube bank have been studied for Cu-water nanofluid with different volume concentration fractions. The effect of the Nanofluids on the heat exchanger performance was studied and compared to that of a conventional fluid. It was found that the heat

transfer enhancement increases with the increase of the volume fraction of the nanoparticle and Reynolds number while there is slight increase in the pressure drop causing an increase in the power requirement.

Keywords: Tube bank; Turbulent flow; Nanofluids ; Forced convection

Nomenclature

A	*Area, [m^2].*	$\dot{V}$	*Volumetric flow rate, [$m^3\ s^{-1}$].*
C_p	*Specific Heat, [$J\ kg^{-1}\ K^{-1}$].*		
C_f	*Skin Friction factor.*		
D	*Pipe diameter, [m].*	***Greek symbols***	
h	*Heat transfer coefficient [$Wm^{-2}K^{-1}$]*	ε	*Turbulent dissipation energy, [$m^2\ s^{-3}$].*
I	*Turbulent intensity.*	φ	*Volume fraction, (%).*
k	*Thermal conductivity, [$W\ m^{-1}\ K^{-1}$].*	ν	*Momentum diffusivity, [$m^2\ s^{-1}$].*
k	*turbulent kinetic energy, [W].*	ρ	*Density, [$kg\ m^{-3}$]*
Nu	*Nusselt number.*	μ	*Dynamic viscosity, [$kg\ m^{-1}\ s^{-1}$].*
P	*Pressure, [Pa].*		
PP	*Pumping power, [W].*	***Subscripts***	
Re	*Reynolds number.*	m	*Mean /average /bulk.*
S_L	*Longitudinal pitch, [m].*	nf	*Nanofluid.*
S_T	*Transverse pitch, [m].*	o	*Base fluid.*
T	*Temperature, [K].*	p	*Nanoparticle.*
U	*Velocity component, [$m\ s^{-1}$].*	t	*Turbulent.*
u'	*Velocity fluctuation, [$m\ s^{-1}$].*	x	*Local / A coordinate.*

Introduction

Forced convection flow over a bank of tubes is of particular importance in the design of heat exchangers. They are the main components in heat transfer system, such as thermal power plants, chemical reactor, air-conditioning equipment, refrigerators, automotive radiators and waste heat recovery technologies. In recent years, the high

cost of energy and material has resulted in an increased effort aimed at producing more efficient heat exchange equipment.

Improving the properties of the heat transfer fluids enhance the heat transfer rate, therefore adding nanoparticles to the working fluids leading to a significant enhancement in thermal performance of heat exchangers. As a result, the size of a heat exchanger can be reduced. Nano fluids which are nano size particles having high thermal conductivity suspended in the base fluid, it was reported to be promising in improvement of thermal and thermo-physical properties of working fluids.

Review of work related to heat transfer characteristic of nanofluids and their diverse application have been reported by Robert Taylor et al [1]. Using nanofluids as working fluids to enhance heat transfer rate have been numerically and experimentally studied by many researchers. Heidary and Kermani [2], Bianco et. al. [3], Kumar and Jagdeesh [4], and Nambura et. al. [5] studied numerically the flow and heat transfer of nanofluids in circular tubes and other different shapes of channels. Different nano particles materials and base fluids were tested. Their results reported that the enhancement of heat transfer mainly depends on Reynolds number and volume fraction of the nano particles and the decreases of the size of nanoparticles. However, this enhancement was accompanied with increasing the pressure drop. Ho et al. [6], Albadr et al. [7], Yin et. al., [8], and Shahrul et. al. [9] investigated experimentally the heat transfer characteristics of nanofluids with different nano particles and base fluids in different experimental facilities including shell and tube heat exchangers under turbulent flow conditions. Their results show that the heat transfer rates were enhanced

compared to base liquid at same mass flow rates and at same inlet temperature.

The heat transfer coefficient of the nanofluid increases with Reynolds number, and the increase of the volume concentration of nanoparticles, however, increasing the volume concentration cause increase in the viscosity of the nanofluid leading to increase in friction factor. Tube bank consists of parallel cylindrical tubes that are heated by the fluid flow normal to it usually arranged in inline or staggered configurations. The fluid flow conditions within the bank are dominated by turbulence because of the induced vortex shedding which enhances the heat transfer process. The turbulence intensity and its generation are determined by the bank geometry and Reynolds number. It has been observed that with lower transverse pitches, the velocity fluctuations become more intensive [10]. Generally, the regimes have been identified from experiment [11], that the flow started to be turbulent at Re > 300. Therefore, a tube bank acts as a turbulent grid and establishes a particular level of turbulence. For this study, in-line tube bank under turbulent flow conditions is investigated.

1. Problem Description and Mathematical Model

The physical domain of flow a round an inline tube bank with five tubes in the flow direction. A configuration is characterized by the tube diameter, (D = 1cm) and longitudinal and transverse pitchesm $S_T = S_L$ = 2D. Because of the symmetry of the tube banks geometry, only a part of the domain needs to be modeled as shown in figure (1). The flow field is considered 5D at the upstream and 10D at the downstream.

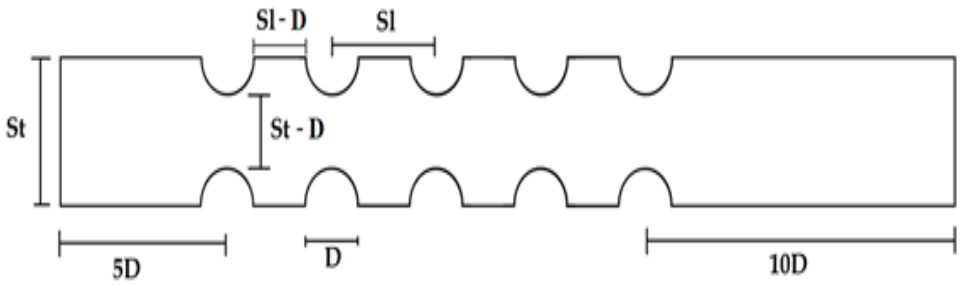

Fig. (1) The computational domain.

The governing equations based on the balance laws of mass momentum and energy and for k - ε turbulence model are given below. The following assumptions were employed :

1. The flow is time-independent (steady-state), two-dimensional, and incompressible.
2. The flow over tube bank is considered turbulent.
3. Heat transfer by radiation and natural convection are neglected.
4. All the thermo-physical properties of water and nanofluids are assumed to be constants.
5. Viscous dissipation is neglected.
6. The base fluid and nano-particles are in thermal equilibrium and no slip between them.
7. A single-phase model was adopted because nanofluids can be considered as Newtonian fluids for low volume concentration fractions, [12].

According to Fluent theory guide [13] the governing equations are :

$$\frac{\partial}{\partial x_i}(\rho u_i) = 0 \quad (1)$$

$$\frac{\partial}{\partial x_j}(\rho u_j u_i) = -\frac{\partial P}{\partial x_i} + \frac{\partial}{\partial x_j}\left[\mu\left(\frac{\partial u_i}{\partial x_j} + \frac{\partial u_j}{\partial x_i} - \frac{2}{3}\delta_{ij}\frac{\partial u_l}{\partial x_l}\right)\right] + \frac{\partial}{\partial x_j}\left(-\rho\overline{u_i' u_j'}\right) \quad (2)$$

$$\frac{\partial}{\partial x_j}\left[u_i\,(\rho E + P)\right] = \frac{\partial}{\partial x_j}\left[\left(k + \frac{C_p \mu_t}{Pr_t}\right)\frac{\partial T}{\partial x_i} + u_i\left(-\rho\overline{u_i' u_j'}\right)\right] \quad (3)$$

$$\frac{\partial}{\partial x_j}\left(\rho u_j k\right) = \frac{\partial}{\partial x_j}\left[\left(\mu + \frac{\mu_t}{\sigma_k}\right)\frac{\partial k}{\partial x_j}\right] + 2\,\mu_t\, S_{ij}.S_{ij} - \beta_1 \rho\varepsilon \quad (4)$$

$$\frac{\partial}{\partial x_j}\left(\rho u_j \varepsilon\right) = \frac{\partial}{\partial x_j}\left[\left(\mu + \frac{\mu_t}{\sigma_\varepsilon}\right)\frac{\partial \varepsilon}{\partial x_j}\right] + 2\,C_{1\varepsilon}\frac{\varepsilon}{k}\,\mu_t\, S_{ij}.S_{ij} - C_{2\varepsilon}\frac{\varepsilon^2}{k} \quad (5)$$

A constant value for the turbulent Prandtl number, Pr_t = 0.85, was used for all the computations.

For the general Reynolds stress tensor, the Boussinesq assumption gives:

$$-\rho\overline{u_i' u_j'} = \mu_t\left(\frac{\partial u_i}{\partial x_j} + \frac{\partial u_j}{\partial x_i}\right) - \frac{2}{3}\left(\rho k + \mu_t\frac{\partial u_l}{\partial x_l}\right)\delta_{ij} \quad (6)$$

Where : δij is the Kronecker delta function (δij=1 if i=j and δij=0 if i≠j), k is the turbulent kinetic energy and μ_t is the turbulent viscosity given by

$$\mu_t = \rho C_\mu\, k^2/\varepsilon \quad (7)$$

The standard values of coefficients for (k-ε) equations are :

C_μ = 0.09 ; σ_k=1.0 ; σ_ε=1.3; $C_{\varepsilon 1}$=1.44; $C_{\varepsilon 2}$=1.92; β_1=1.0

Thermo-physical properties of the nanofluids had been calculated by the relations [14] :

$$\frac{k_{nf}}{k_o} = \frac{\left(k_p + 2\,k_o\right) - 2\,\varphi\left(k_o - k_p\right)}{\left(k_p + 2\,k_o\right) + \varphi\left(k_o - k_p\right)} \quad (8)$$

$$\rho_{nf} = \phi\ \rho_p + (1-\phi)\,\rho_o \quad (9)$$

$$C_{p_{nf}} = \frac{\phi\ \left(\rho C_p\right)_p + (1-\phi)\left(\rho C_p\right)_o}{\rho_{nf}} \quad (10)$$

$$\mu_{nf} = \mu_o\,(1-\phi)^{-2.5} \quad (11)$$

The local convective heat transfer coefficient is determined by

$$h_x = -k\ \frac{(\partial T/\partial n)}{(T_w - T_m)} \quad (12)$$

where T_m is the mean temperature of the heated surface side fluid.

The mean Nu is determined as follows:

$$Nu_m = \frac{h_m D_h}{k} \quad (13)$$

The average heat transfer coefficient is obtained through area averaged integration

$$h_m = \frac{1}{A_s} \int_A h_x \, dA \quad (14)$$

The Reynolds number and the friction factor are defined as follows

$$Re = \frac{\rho u_{in} D_h}{\mu} \quad (15)$$

$$f = 2 \frac{\Delta p}{L} \frac{D_h}{\rho u_{in}^2} \quad (16)$$

The numerical calculations of the average friction factor results are used in calculation of pressure drop. Once the pressure drop (or head loss) is known, the required pumping power to overcome the pressure loss is determined by the relations

$$\Delta P = f \, N_L \, \frac{1}{2} \, \rho (u_{in})^2 \quad (17)$$

$$PP = \dot{V} \, \Delta P \quad (18)$$

Since the governing equations are in spatial coordinates, the boundary conditions were provided for all boundaries of the computation domain as presented in figure (2) :

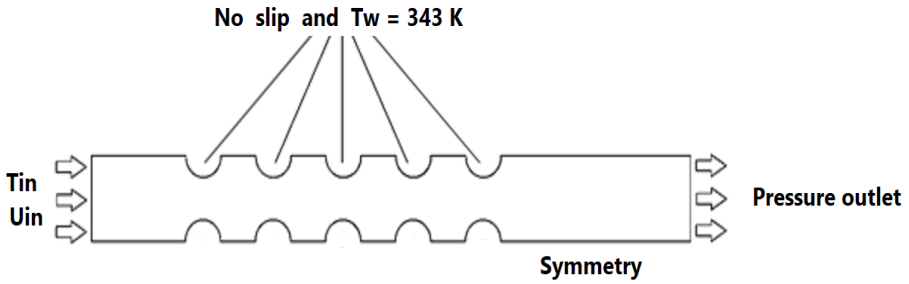

Fig. (2) Boundary conditions on computational domain.

These boundary conditions are :

- **Inlet boundary :**

$$u = u_{in} \ , \ v = w = 0 \ \ and \ T = T_{in} = 300 \ K \qquad (19)$$

The turbulent kinetic energy (k_{in}) and the turbulent dissipation (ε_{in}) are approximated from the turbulent intensity I [15]:

$$k_{in} = \frac{3}{2}(u_{in} I)^2 \qquad \text{and} \quad \varepsilon_{in} = C_{\mu}^{3/4} \frac{k^{3/2}}{L} \qquad (20)$$

The turbulent intensity (I) defined as:

$$I = \frac{u'}{u} \times 100\% \qquad (21)$$

- **Outlet boundary :**

$$P = P_{out} = 0 \qquad (22)$$

- Tubes surfaces

$$u = v = w = 0 \ \ and \ T = T_w = 343 \ K \qquad (23)$$

- Symmetry

$$\frac{\partial u}{\partial y} = \frac{\partial v}{\partial y} = \frac{\partial T}{\partial y} = 0 \qquad (24)$$

2. Numerical Solution and Procedure

The finite volume solver, ANSYS FLUENT 17 is used to obtain the numerical solution of the two-dimensional incompressible Navier–Stokes (RANS) equations. Figure (2) shows an example of a hybrid unstructured grid for the calculation of flow in a tube bank where quadrilateral cells have been used near solid walls to provide better resolution of the viscous effects in the boundary layers and an expanding triangular mesh structure elsewhere.

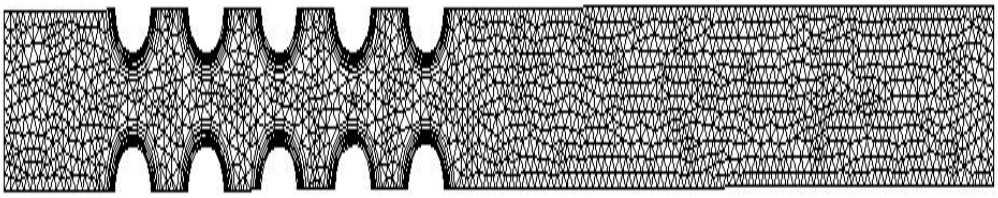

Fig. (3) The computational mesh.

The realizable $k-\varepsilon$ model is adopted because it can provide improved predictions of near-wall flows and flows with high streamline curvature. Solution algorithm with implicit formulation, steady calculation, SIMPLE as the pressure-velocity coupling method, and second-order upwind scheme for energy and momentum equations were selected for simulation. The boundary conditions were specified at the computational domain as given in figure (2). The discritized equations have been solved with residuals of value 10^{-6}. The number of iterations was set to 5000 and calculations start and the iterations continue till the convergence is reached. A case of convergence history is shown in figure (4).

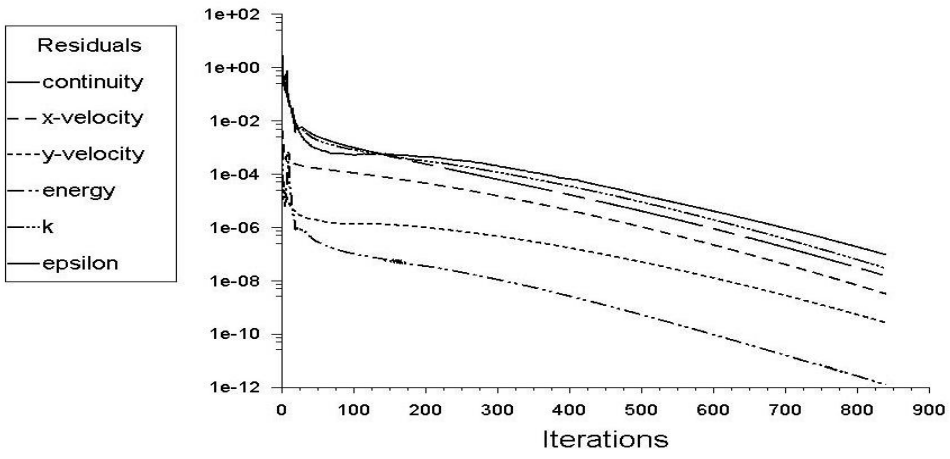

Fig. (4) The convergence history at Re = 750 and 6% Cu-water nanofluid

3. Grid Independence Testing and Model Validation

The grid independence is also verified by calculation of the total heat flux at Re = 1500 for flow over the tube bank with base fluid. The results of different grids shown in figure (5). The grid with 40500 cells has been adopted because it ensured a good compromise between the machine computational time and the accuracy requirements. To ensure the reliability of the simulation methodology, the numerical results of average Nu were compared with the correlation proposed by Zukauskas [16]. These results are shown in figure (6), it reveals good agreement with the experimental results, within maximum deviation 13%, which can be attributed to the discrepancies between the numerical model and experimental model.

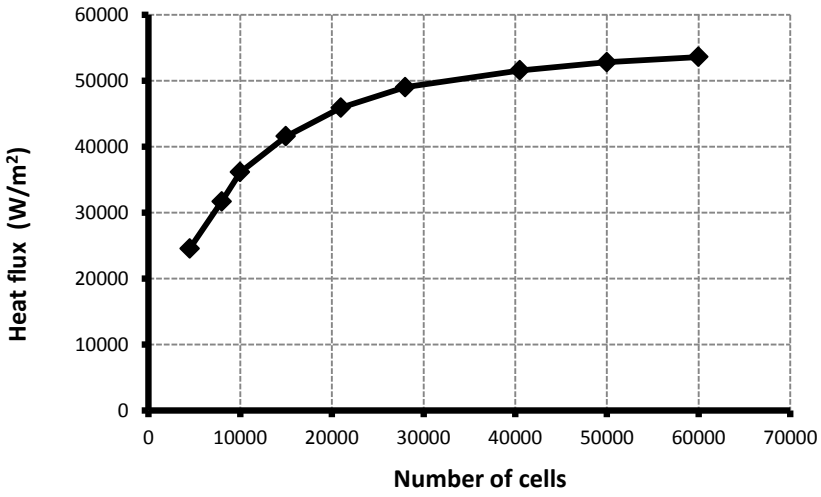

Fig. (5) Grid independence testing

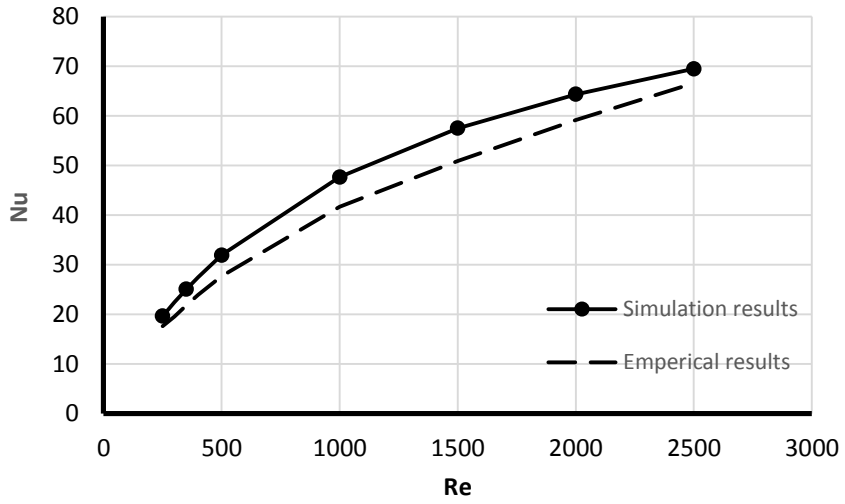

Fig. (6) Comparison between the numerical results and Zukauskas correlation.

4. Results and Discussion

A computational analysis of a two-dimensional turbulent flow past in-line tube bank with nanofluids, is considered in order to evaluate the thermal and fluid-dynamic performances, the results of the simulation analyzed in the following sections. The geometric dimensions kept constant, the range of Reynolds was between 250 and 2500. The Effect of Cu water nanofluid with different volume fractions (φ=0%, 3%, 6%, 9%) on heat transfer enhancement were tested and analyzed.

4.1. Velocity and temperature fields

As shown in figure (7), velocity pattern in the mid-plane of the tubes was observed to be higher and weak near tube surface plane because of the boundary layer development on the surface. a large portion of the tube surface area of only the first rank is exposed to the main flow. A larger flow recirculation region or dead zone is formed between the two adjacent tubes. It also proves clearly the existence of reverse flow patterns upstream of deeper rows.

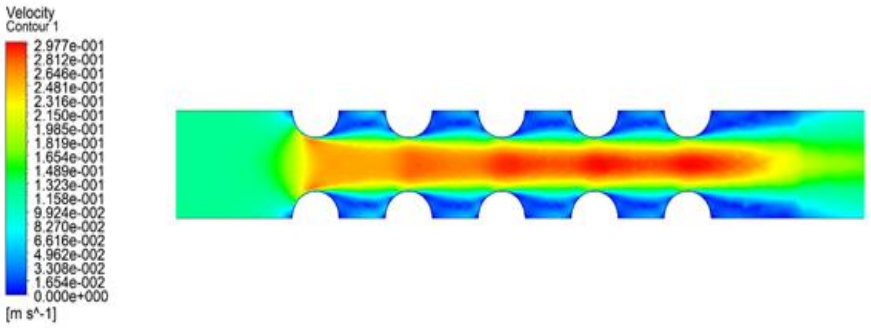

Fig. (7) The velocity fields at Re = 750

Figure (8) shows the temperature distributions within the bank. The cooling rate of the heated element is grater within the tube-mid planes where maximum local velocity occurs. This was evident by the low temperature close to that of the free stream recorded. The temperature gradient near the upstream tube was higher due to the thin boundary layer, while the temperature gradient down stream along the tube is lower than the upstream due to the wake flow.

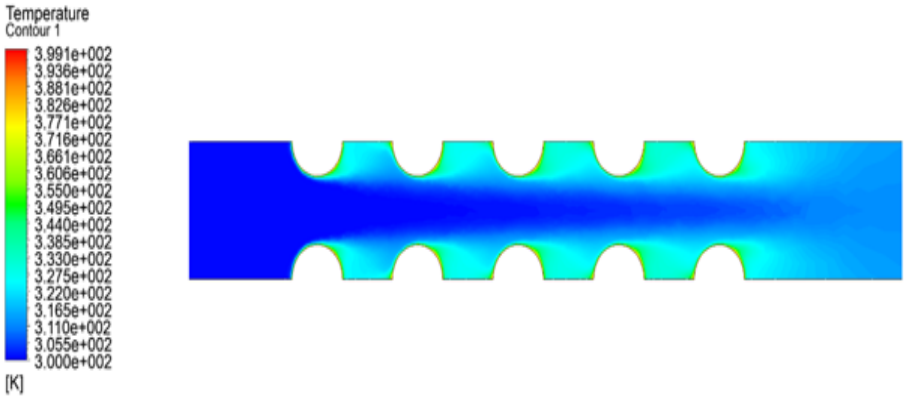

Fig. (8) The temperature contours at Re = 750

4.2. Heat transfer characteristics

The results of simulation reveal that the convective heat transfer coefficient of nanofluid increases with increase in its concentrations. In figure (9), the heat transfer improvement is seen for CuO-water nanofluid from 3%-9% volume fraction. Heat transfer rate increases for a fixed volume fraction of nanofluid with increased Reynolds number and with the increase of volume fraction of nanofluid.

This increase in heat transfer rate is mainly contributed by increase in thermal conductivity of nanofluid by addition of nanoparticles and increased turbulence in the flow. Higher the concentrations of nanoparticles in the base fluid it increases its thermal convection and hence less resistance for heat transfer. This enhancement of the addition of the nanofluid particles for various volume fractions is presented in figure (10), where ratio of ($h_{anaofluid}/h_{base\ fluid}$) plotted against Re number was introduced. The increment ratio is approximately constant versus Reynold number for all volume concentrations.

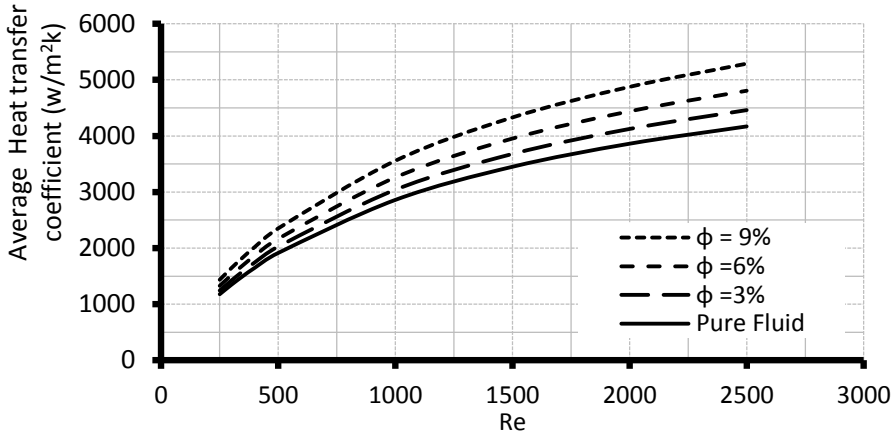

Fig. (9) Heat transfer characteristics of nanofluids Cu/water at different volume concentrations and base fluid.

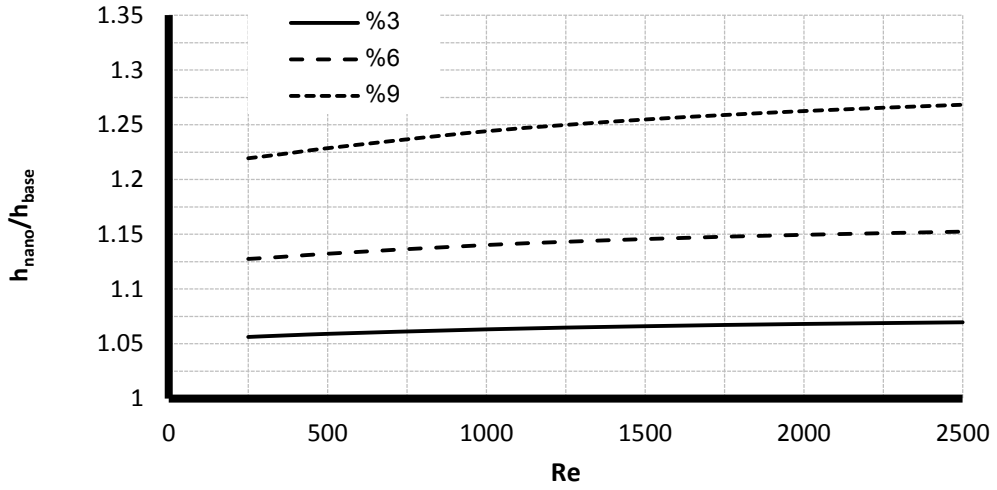

Fig. (10) Heat transfer enhancement of nanofluids Cu/water at different volume concentrations.

4.3. Friction factor and pumping power

The variation of the friction factor for various particle volume fractions of 3, 6 and 9% of Cu/water nanofluid, and for the Reynolds number range from 250 – 2500, were analyzed. The results were shown in figure (11), and reveal that the friction factor is similar for all particle volume fractions where the friction factor decreases with the increase of Reynolds number. It can be stated that the increment of dynamic viscosity due to the presence of the nanoparticles in water, appears to give a slight rise in friction.

The pumping power ratio referred to the base fluid values versus Reynolds number is described in figure (12) for different volume concentrations. It is observed that the ratio (PP_{nf}/PP_o) profiles tend to increase as the volume concentration grows while very little dependence on Re. where the results indicate that pumping power ratio is equal to 1.04, 1.13, and 1.28 for φ = 3%, 6%, and 9%, respectively.

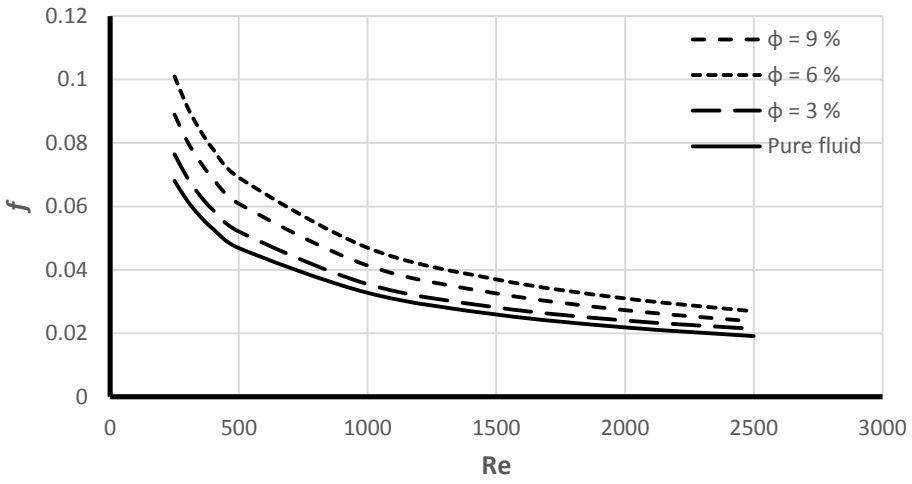

Fig. (11) Friction factor at different of nanofluids at different volume concentrations and base fluid.

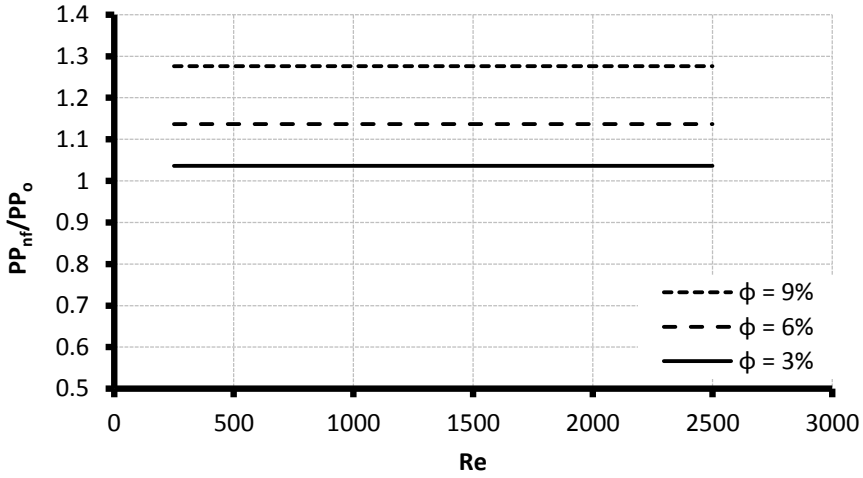

Fig (12) Pumping power requirement ratios for nanofluids at different volume fraction concentrations

5. Conclusions

Simulations for heat transfer under turbulent flow conditions over an inline tube bank with water/ nanofluids have been studied by

ANSYS-FLUENT Software. The Numerical results were reported in forms of heat transfer coefficient and skin friction factor (f) and the main conclusions are summarized as follows:

1. The results showed that nanofluid heat transfer increases as Reynolds number and particles volume concentration increases.
2. Results demonstrated that the increased particle volume fraction improves the heat transfer rates in nanofluids compared to those in the base fluid alone.
3. For nanofluids, increasing the inlet Reynolds number will enhance the convective heat transfer performance and high efficiency with very limited penalties in increased pumping power requirement.

References

[1]. Robert Taylor et al., "Critical review of the novel applications and uses of nanofluids", Poceedings of the ASME 3rd Micro/Nanoscale Heat & Mass Transfer International Conference MNHMT2012 March 3-6 Atlanta, Georgia, USA, (2012).

[2]. Heidary, H., and Kermani, M. J., "Effect of nanoparticles on forced convection in sinusoidal wall channel", Int. Comm. of Heat Mass Transfer, V(37), pp 1520 – 1527, (2012).

[3]. Bianco, V., Manca, O., and Nardini S., "Numerical investigation on nanofluids turbulent convection heat transfer inside circular tube", Int. Journal of Thermal Science, V(50), pp 341 – 349, (2011).

[4]. Kumar V. G., and Jadeesh S., "Investigation of finned tube heat exchanger using nanofluids", ISRD Int. J. Sci. Res. Dev. V(5 - 04), (2017).

[5]. Namburu, P. K., Das, D. K., Tanguturi, K. M., and Vajjha, R. S, "Numerical study of turbulrnt flow and heat transfer characterstics of nanofluids considering variable properties", Int. Journal of Thermal Science V(60), pp 236 – 243, (2012).

[6]. Ho, C. J., Chang C. Y., and Yan, W., "Experimental study of forced convection effectiveness of Al2O3 water nanofluid flowing in circular tubes" Int. commun. Heat and mass transfer V(83), pp 23 – 29, (2017).

[7]. Albadr, J., Satinder T., and Alasadi, M., "Heat transfer through heat exchanger using Al2O3 nanofluid at different concentrations", Case Studies in Thermal Engineering V(1), pp 38–44, (2013).

[8]. Yin, J. L., Wang, D. Z., Cheng, H., & Gu, W. G., "Assessment of RANS to predict flows with large streamline curvature", Materials Sci. and Eng. V(52), pp 1–6. (2013).

[9]. Shahrul O. M., Mahbubul R. S., and Sabri, M., "Experimental investigation on Al2O3 Si O4 and ZnO nano fluids and their applications in a shell and tube heat exchanger", Int. Journal of Heat and Mass Transfer V(97), pp 547 – 558, (2016).

[10]. Yoo, S., Kwon, H., Kim, J., "A study on heat transfer characteristics for staggered tube banks in cross-flow", J. Mech. Sci. Technol. V(21), pp 505 – 512. (2007).

[11]. Zdravkovich, M. M.. Flow around circular cylinders: fundamentals ,First edition. Printed in Oxford University Press, New York. (1997).

[12]. Göktepe, S., Atalik, K., Ertürk, H., "Comparison of single and two-phase models for nanofluid convection at the entrance of a uniformly heated tube", Int. J. Therm. Sci., V(80), pp 83–92, (2014).

[13]. FLUENT theory guide and user manual. (2015).

[14]. Xuan, Y., and Roetzel, W., "Conceptions for heat transfer correlation of nanofluids", International Journal of Heat and Mass Transfer 43 (19), pp 3701-3707, (2000).

[15]. Mohammed H. A, Abed A. M, Wahid M. A., "The effects of geometrical parameters of a corrugated channel with in out-of-phase arrangement", International Communications in Heat and Mass Transfer 40: pp 47-57, (2013).

[16]. Žukauskas, A., & Ulinskas, R. "Efficiency parameters for heat transfer in tube banks", Heat Transfer Engineering, 6(1), pp 19 – 25, (1985).